0026-895X/06/7006-1866–1875
MOLECULAR PHARMACOLOGY
U.S. Government work not protected by U.S. copyright
Mol Pharmacol 70:1866–1875, 2006

Vol. 70, No. 6
26641/3151900
Printed in U.S.A.

Comparison of the Activities of the Truncated Halichondrin B Analog NSC 707389 (E7389) with Those of the Parent Compound and a Proposed Binding Site on Tubulin

Donnette A. Dabydeen, James C. Burnett, Ruoli Bai, Pascal Verdier-Pinard, Sarah J. H. Hickford, George R. Pettit, John W. Blunt, Murray H. G. Munro, Rick Gussio, and Ernest Hamel

Toxicology and Pharmacology Branch (D.A.D., R.B., P.V.-P., E.H.) and Information Technology Branch (R.G.), Developmental Therapeutics Program, Division of Cancer Treatment and Diagnosis, National Cancer Institute at Frederick, National Institutes of Health, Frederick Maryland; Target Structure Based Drug Discovery Group, SAIC-Frederick, Frederick, Maryland (J.C.B.); Department of Chemistry, University of Canterbury, Christchurch, New Zealand (S.J.H.H., J.W.B., M.H.G.M.); and Cancer Research Institute and Department of Chemistry, Arizona State University, Tempe Arizona (G.R.P.)

Received May 16, 2006; accepted August 29, 2006

ABSTRACT

The complex marine natural product halichondrin B was compared with NSC 707389 (E7389), a structurally simplified, synthetic macrocyclic ketone analog, which has been selected for clinical trials in human patients. NSC 707389 was invariably more potent than halichondrin B in its interactions with tubulin. Both compounds inhibited tubulin assembly, inhibited nucleotide exchange on β-tubulin, and were noncompetitive inhibitors of the binding of radiolabeled vinblastine and dolastatin 10 to tubulin. Neither compound seemed to induce an aberrant tubulin assembly reaction, as occurs with vinblastine (tight spirals) or dolastatin 10 (aggregated rings and spirals). We modeled the two compounds into a shared binding site on tubulin consistent with their biochemical properties. Of the two tubulin structures available, we selected for modeling the complex of a stathmin fragment with two tubulin heterodimers with two bound colchicinoid molecules and a single bound vinblastine between the two heterodimers (*Nature (Lond)* **435:**519–522, 2005). Halichondrin B and NSC 707389 fit snugly between the two heterodimers adjacent to the exchangeable site nucleotide. Fitting the compounds into this site, which was also close to the vinblastine site, resulted in enough movement of amino acid residues at the vinblastine site to cause the latter compound to bind less well to tubulin. The model suggests that halichondrin B and NSC 707389 most likely form highly unstable, small aberrant tubulin polymers rather than the massive stable structures observed with vinca alkaloids and antimitotic peptides.

From a structural viewpoint, halichondrin B (Fig. 1) is one of the most complex of the antitubulin compounds. Isolated from the sponges *Halichondria okadai* (Hirata and Uemura, 1986), *Axinella* species (Pettit et al., 1991), and *Lissodendoryx* species (Litaudon et al., 1997), halichondrin B is a potent antimitotic agent that inhibits tubulin assembly (Bai et al., 1991). Because it inhibits the binding of radiolabeled vinblastine to tubulin in a noncompetitive manner, halichondrin B seems to bind in the "vinca domain" rather than in the same site on tubulin as the vinca alkaloids. Like most vinca domain drugs, halichondrin B inhibits both nucleotide exchange on β-tubulin (Bai et al., 1991) and formation of a cross-link between β-tubulin residues Cys12 and, probably, Cys211 (Ludueña et al., 1993). These properties have led to the assumption that the vinca domain was located near the exchangeable nucleotide site at the plus-end of the αβ-tubulin heterodimer, as defined in the electron crystallographic tubulin model (Nogales et al., 1998), in which Cys12 is only a few angstroms from the guanine residue of the exchangeable GDP. The recent success in locating the vinca site using crystals of two αβ-tubulin-colchicinoid complexes bound to a

This work was partially supported by National Cancer Institute contract number NO-1-CO-12400.
Article, publication date, and citation information can be found at http://molpharm.aspetjournals.org.
doi:10.1124/mol.106.026641.

ABBREVIATIONS: NCI, National Cancer Institute; NSC 707389, CA index: 11,15:18,21:24,28-triepoxy-7,9-ethano-12,15-methano-9*H*,15*H*-furo[3,2-*i*]furo[2′,3′:5,6]pyrano[4,3-b][1,4]dioxacyclopentacosin-5-(4*H*)-one, 2-[(2*S*)-3-amino-2-hydroxypropyl]hexacosahydro-3-methoxy-26-methyl-20,27-bis(methylene)-, (2*R*,3*R*,3a*S*,7*R*,8a*S*,9*S*,10a*R*,11*S*,12*R*,13a*R*,13b*S*,15*S*,18*S*,21*S*,24*S*,26*R*,28*R*,29a*S*)-, methanesulfonate (salt); PDB, Protein Data Bank; MES, 4-morpholineethanesulfonate; HPLC, high-performance liquid chromatography; TP-TF, tetrahydropyran-tetrahydrofuran.

stathmin fragment confirmed this hypothesis. However, in these crystals, a single vinblastine molecule bound at the interface between the two tubulin heterodimers, and the adjacent α-tubulin made a major contribution to the binding site (Gigant et al., 2005). Thus, the vinblastine site was shared between the plus-end β-subunit of one heterodimer and the minus-end α-subunit of its neighbor, consistent with the isodesmic tubulin assembly reaction induced by the drug (Timasheff et al., 1991) and with an early photoaffinity-labeling study (Safa et al., 1987). In contrast to the vinca alkaloids and most peptide and depsipeptide antimitotic agents, halichondrin B does not induce a readily detectable aberrant tubulin assembly reaction. Likewise, there does not seem to be an aberrant assembly reaction induced by three vinca site drugs (maytansine, rhizoxin, and disorazol A) or by another noncompetitive inhibitor of vinca alkaloid binding (spongistatin 1) and its analogs. These findings imply that some compounds may bind to the β-tubulin portion of the vinca domain without participation of the α-subunit of another heterodimer. On the other hand, the aberrant assembly products produced by some agents may be of relatively small size or even unstable under the experimental conditions used to study the inhibition of binding of radiolabeled ligands.

Although not the most potent inhibitor of cell growth that binds to tubulin, halichondrin B is nonetheless quite inhibitory. Most cell lines in the NCI drug screen (http://dtp.nci.nih.gov/) yielded IC_{50} values lower than 100 pM, and in animal tumor models, the compound showed excellent activity (Fodstad et al., 1996). In anticipation of clinical trials, a large-scale purification of halichondrin B from *Lissodendoryx* species sponges was undertaken.

Meanwhile, halichondrin B was synthesized de novo (Aicher et al., 1992), and this work led to syntheses of multiple "truncated" analogs (Littlefield et al., 2001; Seletsky et al., 2004; Zheng et al., 2004), including the macrocyclic ketone analog NSC 707389 (also known as E7389 and previously as ER-086526; Fig. 1). This compound, too, showed impressive cytotoxic activity (Towle et al., 2001; Kuznetsov et al., 2004) comparable with that of halichondrin B in the NCI cell screen (http://dtp.nci.nih.gov/). NSC 707389 had excellent antitumor activity in animal models, displayed cellular effects expected of an antitubulin drug, and inhibited tubulin assembly (Towle et al., 2001). NSC 707389 is presently in clinical trials, having replaced halichondrin B as the lead candidate of this chemotype, in part because of potential supply problems with the natural product.

In the studies presented here, we examined the biochemical mechanism of action of NSC 707389 in greater detail and in a direct comparison with halichondrin B. We found the synthetic compound to be more potent than halichondrin B in all assays. In concert with the biochemical data presented here, the specific structural features of NSC 707389 and halichondrin B were used to perform detailed molecular modeling studies of their potential binding site on tubulin.

Materials and Methods

Materials. Halichondrin B was obtained from *Lissodendoryx* species sponges (Litaudon et al., 1997), and dolastatin 10 (Pettit et al.,

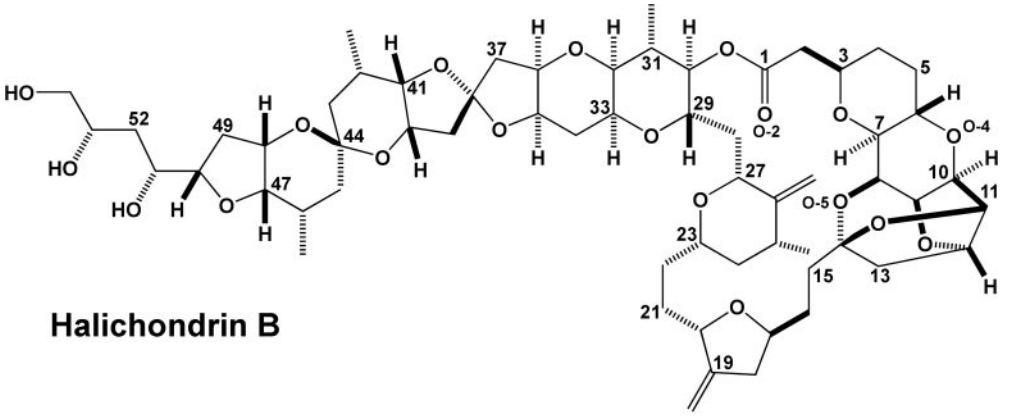

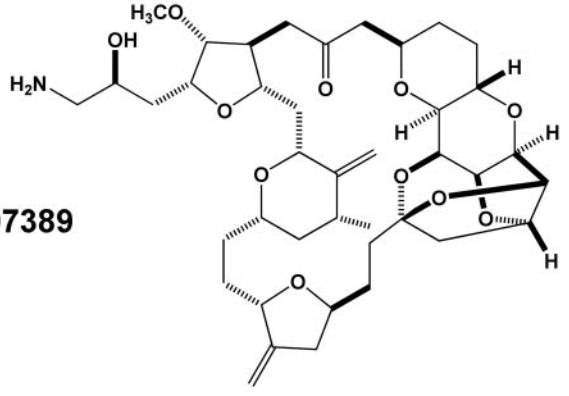

Fig. 1. Molecular structures of halichondrin B and NSC 707389. Numbering is as in Hirata and Uemura (1986) and Uemura et al. (1985).

1989) was synthesized as described previously. NSC 707839 (Littlefield et al., 2001; Zheng et al., 2004) was provided generously by the Eisai Research Institute (Andover, MA). Electrophoretically homogeneous bovine brain tubulin was prepared as described previously (Hamel and Lin, 1984), as was tubulin with [8-^{14}C]GDP bound in the exchangeable site (Duanmu et al., 1986), referred to, respectively, as appropriate, as tubulin-GDP and tubulin-[8-^{14}C]GDP. Both tubulin preparations were passed through Sephadex G-50 (superfine) columns to remove unbound nucleotide and concentrated by precipitation with monosodium glutamate (Grover and Hamel, 1994). [^{3}H]Vinblastine was obtained from GE Healthcare (Little Chalfont, Buckinghamshire, UK), [^{3}H]colchicine from PerkinElmer Life and Analytical Sciences (Boston, MA), and [8-^{14}C]GTP from Moravek Biochemicals (Brea, CA) (repurified to >98% purity by anion exchange chromatography on DEAE-cellulose). [^{3}H]Dolastatin 10 was provided by the Drug Synthesis and Chemistry Branch of the NCI (Bethesda, MD). Human Burkitt lymphoma CA46 cells were obtained from the American Type Culture Collection (Manassas, VA). Three human leukemia cell lines and three monolayer cancer cell lines were provided generously by the Screening Technologies Branch of the NCI (Frederick, MD). Three human primary endothelial cell lines and the culture medium and medium supplements in which they were grown were purchased from Cambrex Bio Science Walkersville, Inc. (Walkersville, MD).

Biochemical Methods. Tubulin assembly was followed by turbidimetry at 350 nm in Beckman Coulter (Fullerton, CA) recording spectrophotometers (models DU 7400 and DU 7500) as described previously (Hamel, 2003). Reaction mixtures contained 10 μM (1.0 mg/ml) tubulin, 0.8 M monosodium glutamate (taken from a 2 M stock solution adjusted to pH 6.6 with HCl), varying drug concentrations, 4% (v/v) dimethyl sulfoxide (as drug solvent), and 0.4 mM GTP. A drug-tubulin preincubation occurred before the addition of GTP. Preincubation (15 min) and incubation (20 min) temperature was 30°C.

Binding of [^{3}H]colchicine was measured using the DEAE-cellulose filter method, as described by Ludueña et al. (1989). Binding of all other radiolabeled ligands was measured by centrifugal gel filtration using 1-ml columns of Sephadex G-50 (superfine) swollen in a solution containing 0.1 M MES (taken from a 1 M stock solution adjusted to pH 6.9 with NaOH) and 0.5 mM $MgCl_2$ and prepared in tuberculin syringe barrels. Unless indicated otherwise, in these experiments, reaction mixtures also contained 0.1 M MES, pH 6.9 (as above), and 0.5 mM $MgCl_2$. Dimethyl sulfoxide, tubulin, and drug concentrations were as indicated in the individual experiments.

Formation of drug-induced oligomers was evaluated by HPLC size-exclusion chromatography with an Agilent (Palo Alto, CA) Series 1100 system. A Shodex Protein KW-802.5 column (80 × 300 mm; Thompson Instruments, Oceanside, CA), protected with a KW-G (6 × 50 mm) guard column, was used. The column was equilibrated and developed with the 0.1 M MES/0.5 mM $MgCl_2$ buffer solution at room temperature (21–22°C), and the flow rate was 1.0 ml/min. Samples (50 μl), before application to the column, were incubated for 30 min at room temperature and contained 2.5 μM tubulin, 0.1 M MES, pH 6.9, 0.5 mM $MgCl_2$, 1% dimethyl sulfoxide (as drug solvent), and drugs as indicated.

Cytological Methods. The leukemia and Burkitt lymphoma cells were grown in suspension cultures in RPMI 1640 medium supplemented with 2 mM L-glutamine and 5% bovine fetal calf serum. The monolayer cancer cell lines were grown in 96-well microtiter plates in RPMI 1640 medium supplemented with 10% fetal calf serum. The primary human endothelial cell lines were cultured as monolayers as recommended by the supplier in 96-well microtiter plates. All cells were grown at 37°C in a humidified atmosphere containing 5% CO_2. For cells grown in suspension culture, drug effects on the increase in cell number were measured. For cells grown in monolayer culture, drug effects on the increase in cell protein were measured with sulforhodamine B.

Molecular Modeling. Insight II (Accelrys, San Diego, CA) was used to visualize and build the models. Discover 2.9, implemented as a module in Insight II, was used for all energy refinements and dynamics simulations, applying the cff91 force field. The HiNT program (eduSoft, LC, Richmond, VA), also implemented as a module in Insight II, was used to evaluate model quality based on the quantitation of intermolecular contacts, as described by Nguyen et al. (2005). In brief, HiNT scores the hydropathicity of a protein-ligand interaction by quantitating all atom-atom interactions between the two species. These interactions include both unfavorable (hydrophobic-polar, base-base, and acid-acid) and favorable (hydrophobic-hydrophobic, hydrogen bonds, and acid-base) contacts. HiNT parameter settings used during these studies were as follows: steric term = Lennard-Jones 6–9 (for cff91 compatibility); lone pair vector focusing = 10; and distance dependence atom-atom interactions = $\exp(-1/r)$.

The X-ray cocrystal structure of two tubulin heterodimers complexed with the RB3 stathmin-like domain with two molecules of bound colchicinoid [*N*-deacetyl-*N*-(2-mercaptoacetyl)-colchicine] and one molecule of bound vinblastine (Gigant et al., 2005) was used for protein coordinates (PDB entry 1Z2B). Only the minus-end α- and plus-end β-subunit, both of which interact with vinblastine, were retained for modeling purposes, along with the exchangeable GDP bound to the β-subunit and the bound vinblastine moiety. The RB3 stathmin fragment, the other two tubulin subunits, the colchicinoid molecules, and the nonexchangeable GTP bound to the minus-end α-tubulin were removed. Although the vinblastine molecule was retained in its original coordinate space, it was decoupled from the internal terms of the potential energy calculations during the docking of halichondrin B and NSC 707389 into their proposed binding sites. In addition, residues not included in the X-ray structure at the α-β-subunit interface of interest were built into the model, and a magnesium ion was positioned in close proximity to the diphosphate of the exchangeable GDP using X-ray crystal structure PDB entry 1SA0 (Ravelli et al., 2004) as a template.

The structures of halichondrin B and NSC 707389 were built using coordinates from the X-ray crystal structure of norhalichondrin A *p*-bromophenacyl ester (Uemura et al., 1985) (Cambridge Structural Database entry DAPRUH). Potentials were assigned to analogous nonhydrogen atoms shared by norhalichondrin A *p*-bromophenacyl ester, halichondrin B, and NSC 707389, so that during molecular mechanics simulations, root-mean-square deviations were minimized, and the stereochemistry remained unchanged. Conformational isomers were generated to explore steric and chemical complementarity between the ligand and protein surfaces. This was achieved by using a molecular dynamics simulation using the cff91 force field. First, both ligands were energy minimized until the norm of the gradient was 0.001 kcal/Å. Next, temperatures were slowly increased by 25 K increments (starting at 0 K), until the target simulation temperature of 300 K was attained. Once the target temperature was reached, the simulations were initiated with an equilibration phase using direct velocity scaling for 10 ps and a time step of 0.5 fs. Thereafter, the Berendsen method of temperature-bath coupling was applied for 100 ps, with a structure collected every 100 fs (Giannakakou et al., 2000).

Both conformational analysis and the energy refinement strategy used during the docking of halichondrin B and NSC 707389 have been well-described previously (Giannakakou et al., 2000; Gussio et al., 2000; Burnett et al., 2003; McGrath et al., 2005; Nguyen et al., 2005). For energy refinements, the protocol involved applying 2000 kcal/mol/Å^2 of force that was stepped off the conformational isomer of the ligand and protein in 100 kcal/mol decrements, followed by optimization with conjugate gradients until the norm of the gradient was 0.01 kcal/Å. This process was applied until all external force was removed. Compound models (energetically and hydropathically feasible conformational isomers of each ligand) were docked in the energy refined tubulin structure using an intermolecular cutoff distance of 0.25 Å. Atom-atom interactions between protein and ligand

were analyzed using the HiNT program. Unfavorable tubulin-ligand contacts were removed using rounds of translational, rotational, and torsional adjustments, followed by tethered minimizations. To evaluate and attain the most desolvated docked models of the ligands, the complexes were layered with a 6 Å solvent shell, and hydrogens of the solvent shell were minimized until the norm of the gradient was 0.001 kcal/Å. This was followed by energy refinement of the entire complex, as described above, until the norm of the gradient was 0.001 kcal/Å. The only complexes accepted were those with the side chains and backbone of the tubulin portion of the models falling within experimentally determined X-ray crystallographic resolution.[1]

Results

Biochemical Comparison of NSC 707389 with Halichondrin B. First, we compared the activities of halichondrin B and NSC 707389 as inhibitors of the assembly of purified tubulin in a reaction dependent on glutamate and GTP (Hamel, 2003). In this direct comparison, the analog was 30 to 40% more potent than the natural product, for we obtained IC_{50} values of 1.4 ± 0.1 μM (S.E.M.) for NSC 707389 and 1.9 ± 0.1 μM for halichondrin B.

We next compared the effects of the two compounds on the binding of [8-^{14}C]GTP, [^{3}H]vinblastine, and [^{3}H]dolastatin 10 to tubulin. These studies were initially performed across a concentration range (Fig. 2) with each radiolabeled ligand. NSC 707389 was more effective as an inhibitor of binding than was halichondrin B in all three assays. Average IC_{50} values in these experiments were 5 μM for NSC 707389 and 28 μM for halichondrin B versus GTP; 13 μM for NSC 707389 and 38 μM for halichondrin B versus vinblastine; and 49 μM for NSC 707389 and >60 μM for halichondrin B versus dolastatin 10.

Near-complete inhibition of GTP binding by both compounds at 60 μM (Fig. 2A) suggests that tubulin is saturated with either compound at this concentration. In contrast, inhibition by both compounds of binding of vinblastine (Fig. 2B) or dolastatin 10 (Fig. 2C) was incomplete at 60 μM, as is typical for noncompetitive inhibition (see below). The observed inhibitory plateaus suggest that when tubulin is saturated with halichondrin B or NSC 707389, affinity in both cases for vinblastine is reduced approximately 75%, whereas for dolastatin 10, affinity was reduced only approximately 25% with halichondrin B and approximately 50 to 60% with NSC 707389.

We have shown with halichondrin B that inhibition of GTP binding was caused by the polyether's inhibiting nucleotide exchange, not by actually binding in the exchangeable site (Bai et al., 1991). This was done by showing that halichondrin B, like virtually all other vinca domain drugs, prevented dissociation of prebound [8-^{14}C]GDP from the exchangeable site in the presence of excess GTP. This experiment was performed with NSC 707389, in comparison with halichondrin B, and a similar result was obtained, as shown in Fig. 3. NSC 707389 was significantly more active than halichondrin B in preventing displacement of [8-^{14}C]GDP from the exchangeable site by exogenous GTP just as it had been in inhibiting binding of [8-^{14}C]GTP to tubulin-GDP (Fig. 2A). In control experiments, in the absence of any drug, dilution of the stock tubulin-[8-^{14}C]GDP solution to 5 μM and its chromatography on the syringe columns resulted in recovery of 0.65 mol of [8-^{14}C]GDP bound per mol of tubulin. The addition of 50 μM concentration of nonradiolabeled GTP to the 5

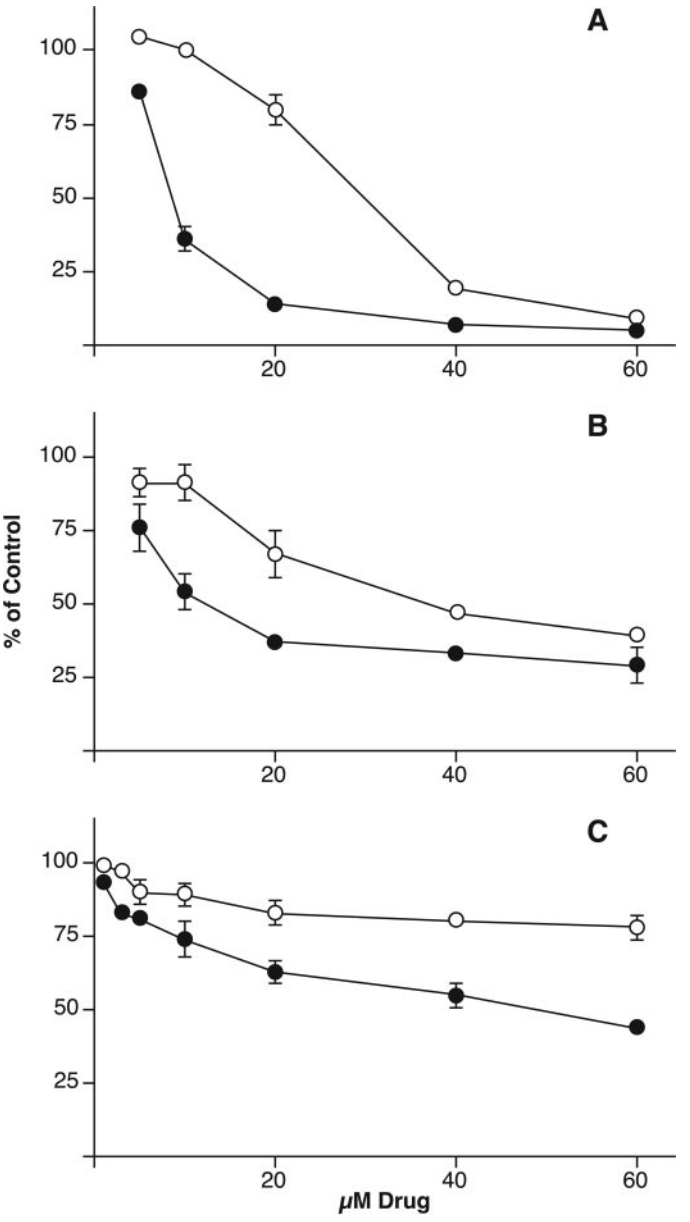

Fig. 2. Comparison of the inhibitory effects of NSC 707389 (●) with those of halichondrin B (○) on the binding of [8-^{14}C]GTP (A), [^{3}H]vinblastine (B), and [^{3}H]dolastatin 10 (C) to tubulin. Each reaction mixture contained 10 μM tubulin, except in the dolastatin 10 binding experiments, in which 5.0 μM tubulin was used, 0.1 M MES, 0.5 mM $MgCl_2$, 1% dimethyl sulfoxide (as drug solvent), and drugs as indicated. Radiolabeled ligand concentrations were 50 μM for GTP (A), 10 μM for vinblastine (B), and 5.0 μM for dolastatin 10 (C). Incubation was for 30 min at room temperature for vinblastine and dolastatin 10 binding and on ice for GTP binding. In the GTP binding experiments, observation of an inhibitory effect requires that drug be added to tubulin before the nucleotide so the [8-^{14}C]GTP was the last component added to the reaction mixtures. Reaction volume was 0.3 ml, and 0.15-ml aliquots were applied to duplicate syringe columns. Samples were applied to room temperature columns, and centrifugation was at room temperature in the vinblastine and dolastatin 10 binding studies. In the GTP binding studies, application of samples to columns and centrifugation were performed at 4°C. Stoichiometry of binding in control reaction mixtures: 0.64 mol GTP/mol tubulin; 0.34 mol vinblastine/mol tubulin; and 0.31 mol dolastatin 10/mol tubulin.

[1] Further details of the modeling studies, including coordinates, can be obtained from R. Gussio (gussio@ncifcrf.gov).

μM tubulin-[8-^{14}C]GDP resulted in the recovery of 0.04 mol of [8-^{14}C]GDP bound per mol of tubulin. We also compared NSC 707389 and halichondrin B as inhibitors of tubulin-dependent GTP hydrolysis and obtained a similar result: under the reaction conditions used, the analog yielded an IC_{50} value of approximately 10 μM, the natural product of approximately 18 μM (data not presented).

Earlier we had found that halichondrin B was a noncompetitive inhibitor of the binding of [^{3}H]vinblastine to tubulin and obtained an apparent K_i value of 5 μM (Bai et al., 1991). Under the same reaction conditions, we examined NSC 707389 at multiple vinblastine and inhibitor concentrations and obtained a comparable result (Fig. 4). The data shown in Fig. 4 are plotted in the Hanes format (Dixon et al., 1979), with competitive inhibition indicated by a family of parallel lines at different inhibitor concentrations and noncompetitive inhibition by a family of lines intersecting on the negative abscissa. These data are most consistent with NSC 707389 being a noncompetitive inhibitor. Dixon analysis of the data shown in Fig. 4 and of data obtained in other experiments yielded an apparent K_i value of 1.9 $\pm$ 0.1 μM (S.D.) for NSC 707389, consistent with the 5 μM obtained previously (Bai et al., 1991) for the less active halichondrin B.

In studies with the spongistatin family of compounds, which seem to be structurally related to the halichondrins, we found one of the most potent, spongistatin 1, to be a noncompetitive inhibitor of dolastatin 10 binding to tubulin. We have not evaluated halichondrin B in detail because of its weak inhibitory effects on dolastatin 10 binding (Fig. 2C), but the stronger activity of NSC 707389 led us to evaluate its effects at multiple concentrations (Fig. 5). Hanes analysis of these data are most consistent with NSC 707389 acting as a noncompetitive inhibitor of dolastatin 10 binding, as was the case with the still more potent spongistatin 1. Dixon analysis of the experiment shown in Fig. 5, and of data obtained in other experiments, yielded an apparent K_i value of 3.4 $\pm$ 0.6 μM (S.D.) for NSC 707389. The more potent spongistatin 1 yielded an apparent K_i value of 0.6 μM in the previous study (Bai et al., 1995a).

Halichondrin B has been evaluated for its ability to cause aberrant tubulin assembly by a number of methods, but no evidence for such reactions has yet been obtained. NSC 707389 has a similar inability, and HPLC gel filtration studies are shown in Fig. 6. As demonstrated previously (Bai et al., 1995b), dolastatin 10 caused a concentration-dependent shift of the tubulin peak (Fig. 6, B–D; 2–10 μM dolastatin 10) from the 100-kDa position to the void volume (structures >400 kDa). Even much higher concentrations of either halichondrin B or NSC 707389 (Fig. 6, E and F, respectively, with the compounds at 100 μM) did not affect the elution pattern of the tubulin.

A number of the vinca domain drugs show a strong ability to stabilize an active conformation of tubulin (Ludueña et al., 1989, 1992; Bai et al., 1990, 1996). We have evaluated this property by examining the ability of this group of drugs to prevent loss of colchicine binding activity during a 3-h preincubation at 37°C. So far, we have found a complete correlation between a drug's ability to induce aberrant polymer formation, as measured by the HPLC method, and its ability to stabilize colchicine binding. Table 1 shows that this generalization extends to NSC 707389, which, like halichondrin B, failed to prevent the loss of tubulin's colchicine binding activity. In this study, maytansine was included as another

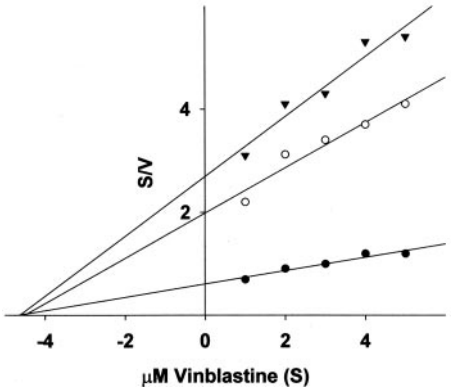

Fig. 4. NSC 707389 inhibits the binding of [^{3}H]vinblastine to tubulin noncompetitively, as shown by Hanes analysis. The studies were performed exactly as described in the Fig. 2 legend for vinblastine binding, except that the concentrations of tubulin and dimethyl sulfoxide were, respectively, 5.0 μM and 2%. The [^{3}H]vinblastine concentrations are shown in the figure; the NSC 707389 concentrations were as follows: (●), none; (○), 6.0 μM; and (▼), 8.0 μM. Ordinate units: micromolar vinblastine × micrograms of tubulin per picomole of vinblastine bound.

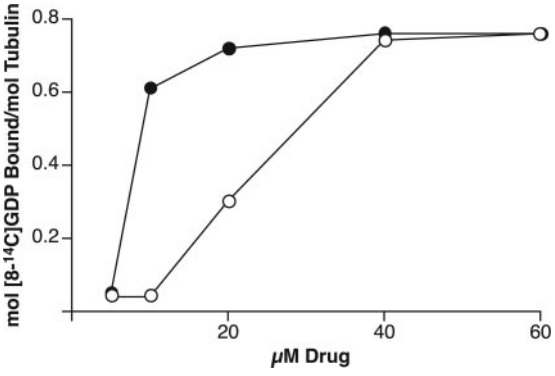

Fig. 3. Comparison of the effects of NSC 707389 (●) and halichondrin B (○) on the ability of nonradiolabeled GTP to displace [8-^{14}C]GDP bound in the exchangeable nucleotide site on tubulin. The study was performed exactly as described for the [8-^{14}C]GTP binding study described in the legend for Fig. 2, except that tubulin-[8-^{14}C]GDP was used instead of tubulin-GDP, and nonradiolabeled GTP was used instead of [8-^{14}C]GTP.

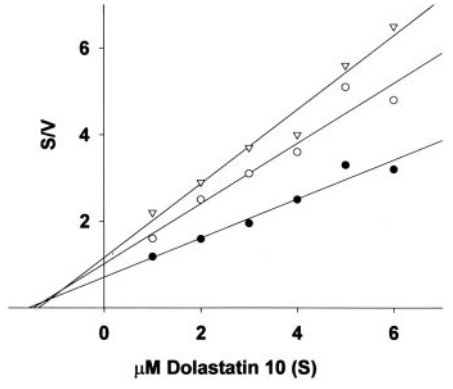

Fig. 5. NSC 707389 inhibits the binding of [^{3}H]dolastatin 10 to tubulin noncompetitively, as shown by Hanes analysis. The studies were performed exactly as described in the Fig. 2 legend for dolastatin 10 binding, except that the concentration of dimethyl sulfoxide was 2%. The [^{3}H]dolastatin 10 concentrations are shown in the figure; the NSC 707389 concentrations were as follows: (●), none; (○), 3.0 μM; and (▽), 6.0 μM. Ordinate units: micromolar dolastatin 10 × micrograms of tubulin per picomole of dolastatin 10 bound.

compound known not to stabilize the colchicine binding activity of tubulin or to induce aberrant polymer formation, and dolastatin 10 was included as a compound that strongly stabilizes the colchicine binding activity of tubulin and, as redemonstrated above, causes formation of aberrant tubulin polymers.

Comparison of the Effects of NSC 707389 and Halichondrin B on the Growth of Human Cancer and Endothelial Cells. We compared the effects of the two compounds on the growth of eight human cancer cell lines (four leukemias, one lymphoma, three solid tumors), and, somewhat surprisingly, in all cases halichondrin B was modestly more active than NSC 707389 (Table 2). The ratios of the IC_{50} values of NSC 707389 to those of halichondrin B varied from 1.3 to 5.0 in these eight lines.

To examine the possibility that NSC 707389, compared with halichondrin B, might have a disproportionate effect on angiogenesis through inhibition of endothelial cell growth, we also examined effects of the two compounds on three primary cultures of human endothelial cells. With these lines, however, halichondrin B was 25- to 50-fold more growth inhibitory than was NSC 707389 (Table 2).

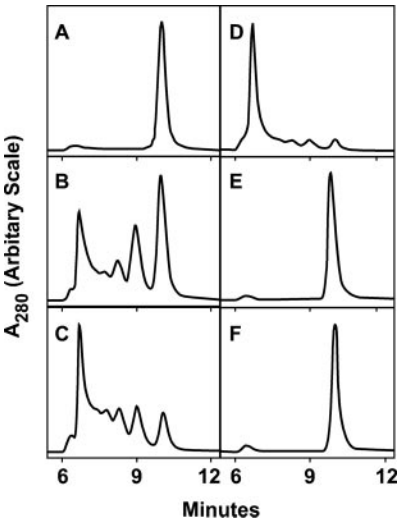

Fig. 6. Dolastatin 10, but not NSC 707389 or halichondrin B, causes a concentration-dependent formation of progressively larger tubulin oligomers. Reaction mixtures contained 10 μM tubulin, 0.1 M MES, 0.5 mM $MgCl_2$, 4% (v/v) dimethyl sulfoxide, and drugs as follows: A, none; B, 2 μM dolastatin 10; C, 5 μM dolastatin 10; D, 10 μM dolastatin 10; E, 100 μM halichondrin B; and F, 100 μM NSC 707389. In A, E, and F, the major protein peak corresponds to 100 kDa, the molecular mass of the $\alpha\beta$-tubulin heterodimer. In D, the major protein peak is in the void volume of the column. Previous studies have shown that the included peaks occur at positions predicted for 100-, 200-, 300-, and 400-kDa species.

TABLE 1

NSC 707389 does not stabilize the colchicine binding activity of tubulin

Each final 100-μl reaction mixture contained, as described by Ludueña et al. (1989), 3.7 μM tubulin, 57 μM [^{3}H]colchicine, 0.1 M MES (pH 6.4 with NaOH in 1 M stock solution), 0.1 mM EDTA, 1 mM GTP, 0.5 mM $MgCl_2$, 1 mM 2-mercaptoethanol, 1 mM EGTA, 5% (v/v) dimethyl sulfoxide, and an additional compound, as indicated, at 40 μM. The preincubation, if performed, was for 3 h at 37°C. At this point the [^{3}H]colchicine was added to the preincubated reaction mixtures. Incubation was for 2 h at 37° C. Average results from two experiments presented in triplicate are presented as colchicine bound (percentage relative to nonpreincubated control).

Drug Added	No Preincubation	Preincubation
	%	
None	100	50
NSC 707389	109	61
Halichondrin B	117	56
Maytansine	115	55
Dolastatin 10	128	133

Molecular Modeling Studies. Docking studies were performed to gain insights into how halichondrin B and NSC 707389 might interact with tubulin. The X-ray crystallographic structure PDB entry 1Z2B (Gigant et al., 2005), reproduced in Fig. 7A without the stathmin fragment, was used for protein coordinates, because this structure includes the binding site for vinblastine on tubulin created by neighboring tubulin heterodimers. Besides the stathmin fragment, the crystal structure contains two $\alpha\beta$-tubulin heterodimers, with GDP bound in the exchangeable sites and GTP in the nonexchangeable sites, along with *N*-deacetyl-*N*-(2-mercaptoacetyl)colchicine bound to each heterodimer and a single vinblastine molecule bound between heterodimers. This structure was chosen because of the inhibitory effects of halichondrin B and NSC 707389 on vinblastine binding and because we wanted to determine whether docking studies could explain the biochemical effects described above, including the greater potency of NSC 707389 compared with the natural product. Only the internal plus-end β-subunit of one heterodimer and the minus-end α-subunit of its neighbor were used in modeling the binding site for halichondrin B (Fig. 7B) and NSC 707389, because only these subunits encompass the vinblastine binding site and, presumably, the vinca domain.

The process of identifying potential binding sites for halichondrin B and NSC 707389 was guided by the biochemical interactions of these compounds with tubulin, with the assumption initially made that the inhibitory effects of these compounds are caused primarily by steric rather than allosteric factors. Thus, as noncompetitive inhibitors of vinblastine binding, halichondrin B and NSC 707389 cannot bind at the same location as vinblastine, but their binding site

TABLE 2

Effects of halichondrin B and NSC 707389 on human tumor and endothelial cell growth

Cells were grown for 72 h in suspension culture or 48 h in monolayer culture. Cells in suspension cultures were counted at 0 time and at the end of the incubation, with the IC_{50} value defined as the compound concentration that reduced increase in cell number by 50% to cultures without drug. Cell growth in monolayer cultures was measured by increase in cell protein, using the sulforhodamine B stain. Average results from at least two experiments are presented. Nanomolar values shown are the IC_{50} ± S.D.

Cell Line	Halichondrin B	NSC 707389	IC_{50} (NSC 707389)/ IC_{50} (halichondrin B)
	nM		
CA46[a]	0.30 ± 0.1	0.70 ± 0.1	2.3
CCRF-CEM[b]	0.90 ± 0.1	2.5 ± 0.5	2.8
K-562[b]	9.0 ± 1	30 ± 3	3.3
MOLT-4[b]	0.20 ± 0.1	0.45 ± 0.07	2.3
RPMI-8226[b]	0.30 ± 0.1	0.40 ± 0.2	1.3
MCF7[c,d]	0.30[e]	1.0[e]	3.3
PC-3[d,f]	0.28 ± 0.09	0.83 ± 0.2	3.0
NCI-H522[d,g]	0.12 ± 0.03	0.60 ± 0.3	5.0
HUVEC[d,h]	0.068 ± 0.01	1.7 ± 0.5	25
HMVEC-L[d,i]	0.49 ± 0.1	23 ± 10	47
HAEC[d,j]	0.070 ± 0.04	3.6 ± 2	51

[a] Human Burkitt lymphoma line, grown in suspension culture.
[b] Human leukemia line, grown in suspension culture.
[c] Human breast carcinoma line.
[d] Grown in monolayer culture.
[e] The same value was obtained in two experiments.
[f] Human prostate carcinoma line.
[g] Human non–small-cell lung carcinoma line.
[h] Human umbilical vein endothelial cells.
[i] Human lung microvascular endothelial cells.
[j] Human aortic endothelial cells.

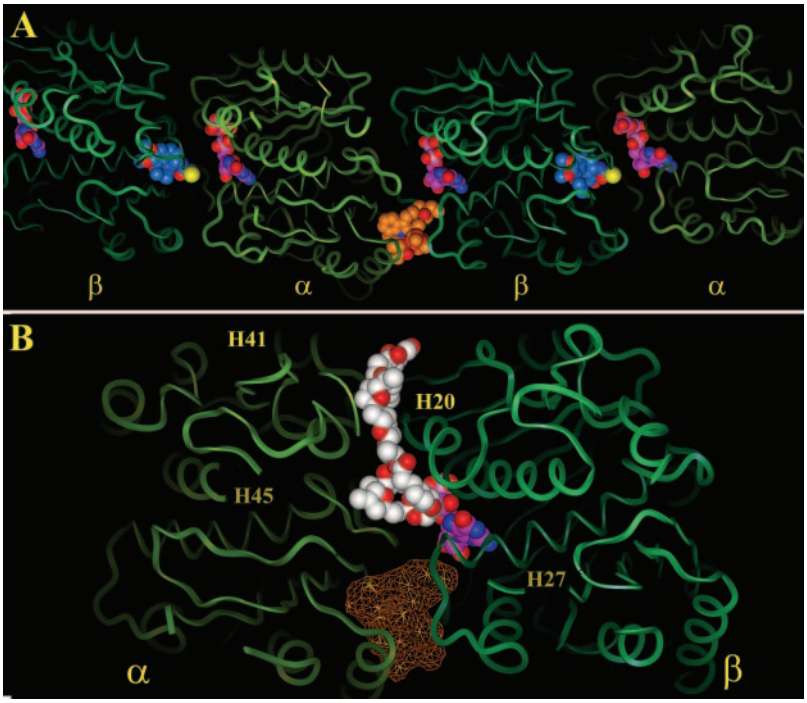

Fig. 7. Global views of the vinblastine and halichondrin B/NSC 707389 binding sites. A, crystal structure of two αβ-tubulin heterodimers with two bound colchicinoid molecules and a single bound vinblastine (Gigant et al., 2005), with the RB3 stathmin fragment removed. Vinblastine, colchicinoid, GTP, and GDP molecules are space-filled. Vinblastine carbons are orange; colchicine, analog blue; and GDP/GTP, magenta (exchangeable site GDP bound to β-tubulin, nonexchangeable site GTP to α-tubulin). Oxygen atoms are red; nitrogen, dark blue; sulfur, yellow; and phosphorous, pink. The α-subunits are yellow-green ribbons, and the β-subunits are blue-green ribbons. B, the minus-end α-subunit/plus-end β-subunit interface with halichondrin B (space-filled; white carbons) docked in its predicted binding site. Other atoms and ribbons are colored as in A. The vinblastine binding site (Gigant et al., 2005) is depicted in orange mesh as a location reference only, because vinblastine and halichondrin B cannot bind simultaneously. The exchangeable GDP on β-tubulin is also shown, but, for greater clarity, the colchicine analog at the β-tubulin minus-end and the nonexchangeable GTP at the α-tubulin plus-end have been deleted.

should be located near the vinblastine site. Furthermore, halichondrin B and NSC 707389 do not bind directly to the exchangeable nucleotide site, but they do prevent nucleotide exchange, making it likely that they interact with tubulin near the exchangeable site.

These considerations led us to examine a deep pocket near the vinblastine site and adjacent to the exchangeable site between the minus-end α-subunit and the plus-end β-subunit in the crystal structure of Gigant et al. (2005), as shown in Fig. 7A. Figure 7B shows halichondrin B docked into this site after the reiterative process described under *Materials and Methods*.

Much like the vinblastine site, the proposed halichondrin B/NSC 707389 pocket is surrounded by both rigid and flexible secondary structural features of tubulin (Fig. 7B). On the α-subunit side, these include 1) a flexible turn located between helices 45 and 46[2]; 2) part of a large flexible loop, including residues Gly43 though Asp47, that shields the binding site from solvent; and 3) a turn between helix 41 and sheet 4(E6). The β-subunit side of the pocket includes 1) helix 20; 2) a portion of a flexible turn leading into helix 27 (Thr223[3] and Gly225); and 3) residues Phe94 and Gly95.

With a suitable ligand binding pocket identified, the first phase of the docking simulations involved identifying feasible binding locations for the relatively rigid, conformationally restricted macrocycles of halichondrin B and NSC 707389. These portions of the ligands exhibited their greatest steric and hydropathic complementarity and maximally desolvated binding modes within the widest and deepest section of the binding pocket. This placed the macrocycles adjacent to the exchangeable nucleotide site. We next focused on halichondrin B, because any sterically and hydropathically feasible binding mode for this ligand must also accommodate its TP-TF extension and terminal glycerol tail. Accommodating the TP-TF/glycerol tail portion of halichondrin B significantly reduced the number of possible macrocyclic conformations that could bind in the proposed tubulin pocket. Nevertheless, it was still necessary to conduct exhaustive rounds of translational, rotational, and torsional adjustments, followed by tethered minimizations and hydropathic evaluations, to obtain the best modeled binding modes for halichondrin B and NSC 707389.

In the best models, shown in Fig. 8, A and C, and Fig. 8, B and D, for halichondrin B and NSC 707389, respectively, the macrocycles of the two compounds attain maximum desolvation via hydrophobic contacts with surrounding residues. These include α-subunit residues Phe244, Ala247, Leu248, and Tyr357 and β-subunit residues Gly81, Pro82, Thr223, and Gly225. (None of these residues interact with vinblastine, as is apparent in Fig. 7B.) In concert with solvent shielding, two of the polar groups, O-4 and O-5 (see also Fig. 1), of the ligands orient toward the solvent; the O-4 atom engages in a favorable acid-base interaction with β-Gln15; the carbonyl oxygen at C-1 (O-2) of each ligand forms a hydrogen bond with the side-chain hydroxyl of β-Ser80.

In the halichondrin B model (Fig. 8A), the TP-TF moiety adopts a conformation that allows it to arch into the groove, which gradually narrows, between the minus-end α-subunit and the plus-end β-subunit. In this region, ligand desolvation is achieved through favorable hydrophobic contacts with the side-chain methyl of α-Thr130, the pyrrolidine of β-Pro72, and the phenyl side chain of β-Phe94 (Fig. 8A). Moreover, the hydroxyl groups of the glycerol tail lock the proposed conformation in place via hydrogen bonds with the backbone carbonyl oxygen atoms of β-Phe94 and β-Gly95 and with the side-chain amide carbonyl oxygen of β-Gln96. For comparison, in the NSC 707389 model (Fig. 8B), the hydroxyl group

[2] The designations of protein secondary structural features are as in PDB entry 1Z2B.

[3] The amino acid residue numbers used for β-tubulin follow the convention in Nogales et al. (1998), which maximized sequence alignment with α-tubulin rather than the actual sequence established by sequencing the polypeptide chain (Krauhs et al., 1981).

of the terminal aminopropanol moiety forms a hydrogen bond with the side-chain carboxylate of α-Asp47, whereas the amino group forms a strong hydrogen bond with the side-chain carboxylate of β-Asp76. Overall, and characteristic of high-quality protein-ligand structures (< 2.0 Å resolution), halichondrin B and NSC 707389 are docked so that they possess optimal steric and electrostatic complementarity with tubulin and minimal solvent exposure, as shown in space-filling models in Fig. 8, C and D.

Finally, the impact of halichondrin B and NSC 707389 binding on the vinblastine site was evaluated. As shown in Figs. 7 and 8, neither docked compound directly interacts with the vinblastine site. However, the proposed halichondrin B/NSC 707389 binding models propagate regional structural changes that would have a negative impact on vinblastine binding. In particular, during halichondrin B/NSC 707389 binding, residues surround the macrocyclic ring and engage in hydrophobic collapse with these ligands to provide a favorable complementary surface. As a consequence of these local structural changes, a concomitant movement in the residues of the vinblastine site occurs, causing a loss in complementarity for vinblastine (Fig. 9), which is consistent with the noncompetitive inhibition observed with halichondrin B and NSC 707389.

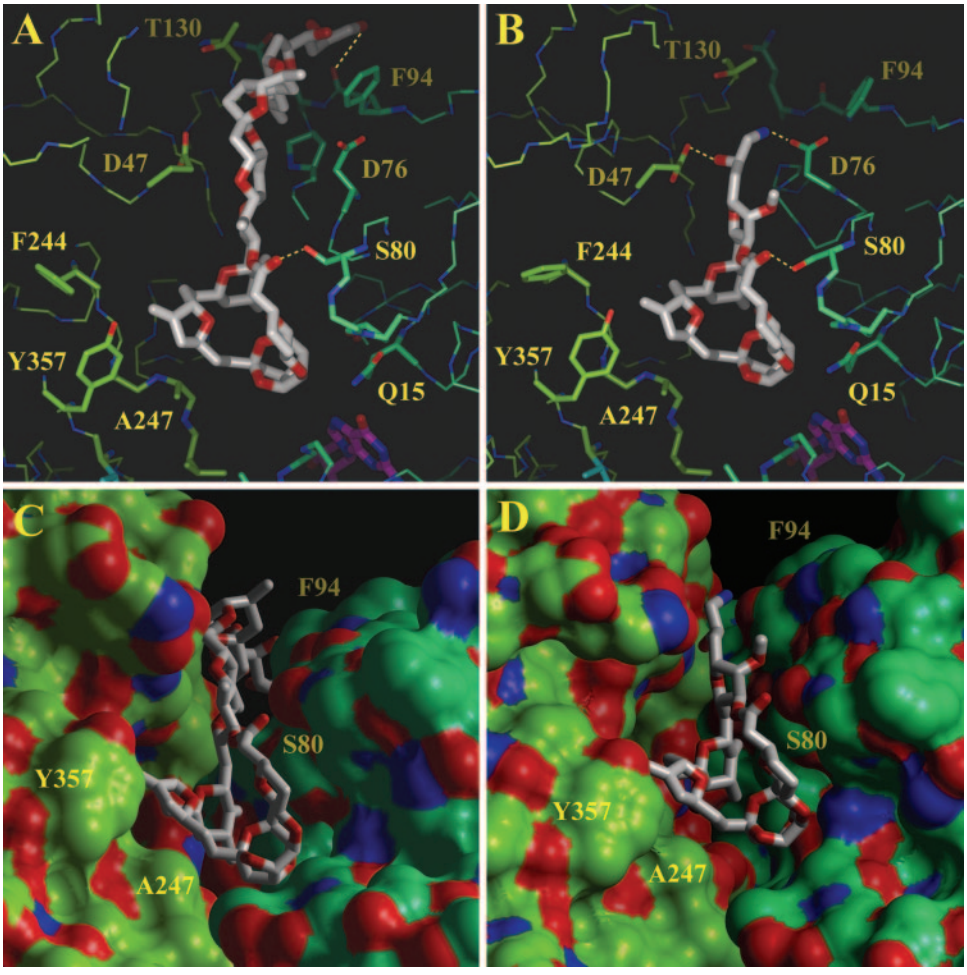

Fig. 8. Close-up views of docked models of halichondrin B (A and C) and NSC 707389 (B and D). Carbon atoms of the α-subunit are yellow-green; of the β-subunit, blue-green; of halichondrin B and NSC 707389, white; and of GDP, magenta. In A and B, halichondrin B, NSC 707389, GDP, and tubulin residues that interact with and/or surround the binding sites of the compounds are shown as thicker sticks than the remainder of the visible residues. All oxygen atoms are red and nitrogen dark blue. Yellow broken lines indicate predicted hydrogen bonds. In C and D, Connolly surfaces of the tubulin subunits are shown to emphasize the depth of binding and high level of desolvation achieved by the proposed binding modes for both halichondrin B and NSC 707389.

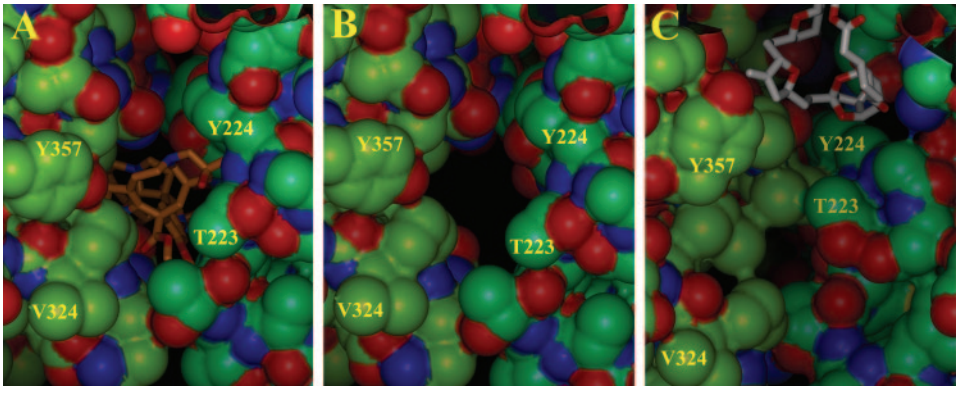

Fig. 9. Steric collapse of the vinblastine site after halichondrin B/NSC 707389 binding. All colors are as described in the legend to Fig. 7. A and B, Connolly surfaces of the vinblastine binding site, with and without the drug, respectively. For comparison, C shows the steric collapse of the vinblastine binding site that occurs when either halichondrin B or NSC 707389 are docked at their predicted binding site.

Discussion

We have found that NSC 707389, a simplified analog of the natural product halichondrin B, is moderately more active than the parent compound as an antitubulin agent at the biochemical level. This was true for every property we examined quantitatively, including inhibition of assembly, nucleotide exchange, [^{3}H]vinblastine binding, and [^{3}H]dolastatin 10 binding. We had initially postulated that the effects of halichondrin B and NSC 707389 on ligand binding were probably caused by steric effects (the bulky halichondrin B and NSC 707389 blocking access to other sites) as opposed to allosteric effects (commonly invoked to explain noncompetitive inhibition).

Our modeling results have caused us to modify this initial assumption, although it remains valid as a rationale for inhibition of nucleotide exchange. The proposed binding models of halichondrin B and NSC 707389 readily explain in steric terms the activity of these compounds as inhibitors of nucleotide exchange. As shown in Fig. 8, A and B, the space occupied by the macrocycles is the only plausible route for nucleotide exit and entry at the exchangeable site. Nucleotide exchange on β-tubulin is believed to involve initial rapid dissociation of the nucleotide bound in the exchangeable site (Brylawski and Caplow, 1983), followed by rapid binding of the incoming nucleotide. The data presented above with tubulin-[8-^{14}C]GDP showed that both compounds interfere with the initial nucleotide release step.

In the case of vinblastine binding, however, the bound models of both halichondrin B and NSC 707389 occupy a different region of the $\alpha\beta$ interface between heterodimers than does vinblastine in the crystal structure (Gigant et al., 2005). Moreover, refinement of the binding of halichondrin B and NSC 707389 at this interface resulted in constricting the vinblastine site so that it no longer was easily accessible to the vinca alkaloid (Fig. 9). The model thus predicts that the polyether macrocycles cause a change in conformation at the vinblastine site. This is clearly inhibition of vinblastine binding because of an allosteric effect on the conformation of tubulin.

Localization, albeit only through molecular modeling, of halichondrin B and NSC 707390 to the interdimer interface predicts that these agents, too, should induce an aberrant tubulin polymerization reaction. However, thus far, we have found no evidence for such a reaction by electron microscopy, turbidimetry, or HPLC, as shown in Fig. 6. This would imply that the binding site for these agents should be solely on β-tubulin. Our studies were all performed with 10 μM tubulin in 0.1 M MES/0.5 mM $MgCl_2$, primarily at room temperature. In contrast, under substantially different reaction conditions, NSC 707389 caused the formation of ill-defined tubulin aggregates (Jordan et al., 2005), observed by electron microscopy. The studies of Jordan et al. (2005) were performed at 37°C, and reaction mixtures contained 10-fold higher tubulin and almost 4-fold higher Mg^{2+} concentrations, microtubule seeds, EGTA, GTP, and a mixture of MES and 1,4-piperazineethanesulfonate buffers. It is not readily obvious which of these difference(s) in reaction conditions account for the different findings regarding aggregate formation. In studies with peptide and depsipeptide antimitotic drugs, we have found aberrant polymer formation to be strongly influenced by reaction temperature, reaction pH, and Mg^{2+} concentration (E. Hamel, unpublished data). Because the HPLC analysis of Fig. 6 was not performed under equilibrium conditions, we tentatively conclude that a higher order binding species for halichondrin B and NSC 707389 must be unstable in 0.1 M MES/0.5 mM $MgCl_2$.

Approaching this question will require ample amounts of active analogs to evaluate stoichiometry of binding and potential assembly reactions under equilibrium conditions. An even more definitive answer might be obtained if stathmin fragment-tubulin-colchicinoid crystals containing bound polyether could be analyzed, as described by Gigant et al. (2005), who introduced vinblastine into the crystals. Our binding model predicts that, like with vinblastine, a single polyether molecule should bind at the heterodimer interface, with major contributions from α-tubulin and β-tubulin from different heterodimers to the binding site.

The binding models help explain why the truncated NSC 707389 is moderately more potent than the larger natural product as an inhibitor of tubulin assembly. The macrocycles of both compounds fit snugly into the cleft between $\alpha\beta$-heterodimers, adjacent to GDP bound in the exchangeable site of the β-subunit. On thermodynamic grounds, especially considering the location of the macrocycle binding pocket, one would anticipate that the smaller NSC 707389 would bind more readily than halichondrin B. In particular, relative molecular size may itself affect binding efficiency. Although the proposed binding modes for both compounds show that each achieves good complementarity and desolvation (Fig. 8), the larger molecule, halichondrin B, has a greater number of accessibility requirements than does NSC 707389. This is particularly true given the number of loops and flexible components present in the proposed binding site. Because proteins are a dynamic ensemble of conformations, the smaller NSC 707389 should possess greater steric access to a common binding site. As one of several possible examples, the α-subunit side of the TP-TF moiety of halichondrin B is shielded from solvent by residues α-Gly43 through α-Asp47. These amino acids are part of a large flexible loop. Its natural movements would result in fewer accessible conformations for halichondrin B than for NSC 707389, which has a minimal interaction with this loop. Moreover, in our models, NSC 707389 forms tighter hydrogen bonds with tubulin compared with halichondrin B. Both the hydroxyl and amino substituents of the terminal aminopropanol moiety of NSC 707389 form strong hydrogen bonds with acidic residues in a portion of the binding pocket that has limited solvent exposure (Fig. 8, B and D). In comparison, the flexible glycerol tail hydroxyl groups of halichondrin B form weaker hydrogen bonds with more solvent-exposed amino acid residues (Fig. 8, A and C).

Finally, we should note that the enhanced activity of NSC 707389 relative to halichondrin B in the tubulin assays was not mirrored in its effects on cell growth. In the eight cancer cell lines we examined, in every case, the natural product was more potent. The differences, however, were not great, and such discrepancies have been observed among many classes of tubulin inhibitors. Nevertheless, we were surprised by this result because NSC 707389 was superior to halichondrin B in NCI in vivo tumor studies (Alley et al., 2005). We speculated that perhaps the superior antitumor activity of NSC 707389 might derive from a differential effect on endothelial cells, because significant vascular effects have been reported with a number of antitubulin drugs. However, in the

three primary endothelial lines we examined, halichondrin B was substantially more inhibitory than NSC 707389. The most likely explanation, therefore, for the greater antitumor activity of the synthetic analog is that it has less toxicity in vivo than the natural product (Alley et al., 2005). This lower toxicity may result from a generally lower sensitivity of non-neoplastic cells to NSC 707389 compared with halichondrin B, as occurred in the primary endothelial lines we examined.

References

Aicher TD, Buszek KR, Fang FG, Forsyth CJ, Jung SH, Kishi Y, Matelich MC, Scola PM, Spero DM, and Yoon SK (1992) Total synthesis of halichondrin B and norhalichondrin B. *J Am Chem Soc* **114:**3162–3164.

Alley MC, Smith AC, Donohoe SJ, Schweikart KM, Newman DJ, and Tomaszewski JE (2005) Comparison of the relative efficacies and toxicities of halichondrin B analogues, in *Proceedings of the AACR-NCI-EORTC Conference on Molecular Targets and Cancer Therapeutics*; 2005 Nov 14–18; Philadelphia, PA, abstract C230, pp 257, American Association for Cancer Research, Philadelphia, PA.

Bai R, Paull KD, Herald CL, Malspeis L, Pettit GR, and Hamel E (1991) Halichondrin B and homohalichondrin B, marine natural products binding in the vinca domain of tubulin: discovery of tubulin-based mechanism of action by analysis of differential cytotoxicity data. *J Biol Chem* **266:**15882–15889.

Bai R, Pettit GR, and Hamel E (1990) Binding of dolastatin 10 to tubulin at a distinct site for peptide antimitotic agents near the exchangeable nucleotide and vinca alkaloid sites. *J Biol Chem* **265:**17141–17149.

Bai R, Schwartz RE, Kepler JA, Pettit GR, and Hamel E (1996) Characterization of the interaction of cryptophycin 1 with tubulin: binding in the *Vinca* domain, competitive inhibition of dolastatin 10 binding, and an unusual aggregation reaction. *Cancer Res* **56:**4398–4406.

Bai R, Taylor GF, Cichacz ZA, Herald CL, Kepler JA, Pettit GR, and Hamel E (1995a) The spongistatins, potently cytotoxic inhibitors of tubulin polymerization, bind in a distinct region of the vinca domain. *Biochemistry* **34:**9714–9719.

Bai R, Taylor GF, Schmidt JM, Williams MD, Kepler JA, Pettit GR, and Hamel E (1995b) Interaction of dolastatin 10 with tubulin: induction of aggregation and binding and dissociation reactions. *Mol Pharmacol* **47:**965–976.

Brylawski BP and Caplow M (1983) Rate of nucleotide release from tubulin. *J Biol Chem* **258:**760–763.

Burnett JC, Schmidt JJ, Stafford RG, Panchal RG, Nguyen TL, Hermone AR, Vennerstrom JL, McGrath CF, Lane DJ, Sausville EA, et al. (2003) Novel small molecule inhibitors of botulinum neurotoxin A metalloprotease activity. *Biochem Biophys Res Commun* **310:**84–93.

Dixon M, Webb EC, Thorne CJR, and Tipton KF (1979) *Enzymes.* Academic Press, New York.

Duanmu C, Lin CM, and Hamel E (1986) Tubulin polymerization with ATP is mediated through the exchangeable GTP site. *Biochim Biophys Acta* **881:**113–123.

Fodstad O, Breistol K, Pettit GR, Shoemaker RH, and Boyd MR (1996) Comparative antitumor activities of halichondrins and vinblastine against human tumor xenografts. *J Exp Ther Oncol* **1:**119–125.

Giannakakou P, Gussio R, Nogales E, Downing KH, Zaharevitz D, Bollbuck B, Poy G, Sackett D, Nicolaou KC, and Fojo T (2000) A common pharmacophore for epothilones and taxanes: molecular basis for drug resistance conferred by tubulin mutations in human cancer cells. *Proc Natl Acad Sci USA* **97:**2904–2909.

Gigant B, Wang C, Ravelli RBG, Roussi F, Steinmetz MO, Curmi PA, Sobel A, and Knossow M (2005) Structural basis for the regulation of tubulin by vinblastine. *Nature (Lond)* **435:**519–522.

Grover S and Hamel E (1994) The magnesium-GTP interaction in microtubule assembly. *Eur J Biochem* **222:**163–172.

Gussio R, Zaharevitz DW, McGrath CF, Pattabiraman N, Kellogg GE, Schultz C, Link A, Kunick C, Leost M, Meijer L, et al. (2000) Structure-based design modifications of the paullone molecular scaffold for cyclin-dependent kinase inhibition. *Anticancer Drug Design* **15:**53–66.

Hamel E (2003) Evaluation of antimitotic agents by quantitative comparisons of their effects on the polymerization of purified tubulin. *Cell Biochem Biophys* **38:**1–21.

Hamel E and Lin CM (1984) Separation of active tubulin and microtubule-associated proteins by ultracentrifugation and isolation of a component causing the formation of microtubule bundles. *Biochemistry* **23:**4173–4184.

Hirata Y and Uemura D (1986) Halichondrins—antitumor polyether macrolides from a marine sponge. *Pure Appl Chem* **58:**701–710.

Jordan MA, Kamath K, Manna T, Okouneva T, Miller HP, Davis C, Littlefield BA, and Wilson L (2005) The primary antimitotic mechanism of action of the synthetic halichondrin E7389 is suppression of microtubule growth. *Mol Cancer Ther* **4:**1086–1095.

Krauhs E, Little M, Kempf T, Hofer-Warbinek R, Ade W, and Ponstingl H (1981) Complete amino acid sequence of β-tubulin from porcine brain. *Proc Natl Acad Sci USA* **78:**4156–4160.

Kuznetsov G, Towle MJ, Cheng H, Kawamura T, TenDyke K, Liu D, Kishi Y, Yu MJ, and Littlefield BA (2004) Induction of morphological and biochemical apoptosis following prolonged mitotic blockage by halichondrin B macrocyclic ketone analog E7389. *Cancer Res* **64:**5760–5766.

Litaudon M, Hickford SJH, Lill RE, Lake RJ, Blunt JW, and Munro MHG (1997) Antitumor polyether macrolides: new and hemisynthetic halichondrins from the New Zealand deep-water sponge *Lissodendoryx* sp. *J Org Chem* **62:**1868–1871.

Littlefield BA, Palme MH, Seletsky BM, Towle MJ, Yu MJ, and Zheng W (2001), inventors, Eisai Co., Ltd., assignee. Macrocyclic analogs and methods of their use and preparation. U.S. patent 6,214,865. 2001 April 10.

Ludueña RF, Prasad V, Roach MC, and Lacey E (1989) The interaction of phomopsin A with bovine brain tubulin. *Arch Biochem Biophys* **272:**32–38.

Ludueña RF, Roach MC, Prasad V, and Pettit GR (1992) Interaction of dolastatin 10 with bovine brain tubulin. *Biochem Pharmacol* **43:**539–543.

Ludueña RF, Roach MC, Prasad V, and Pettit GR (1993) The interaction of halichondrin B and homohalichondrin B with bovine brain tubulin. *Biochem Pharmacol* **45:**421–427.

McGrath CF, Pattabiraman N, Kellogg GE, Lemcke T, Kunick C, Sausville EA, Zaharevitz DW, and Gussio R (2005) Homology model of the CDK1/cyclin B complex. *J Biomol Struct Dyn* **22:**493–502.

Nguyen TL, McGrath C, Hermone AR, Burnett JC, Zaharevitz DW, Day BW, Wipf P, Hamel E, and Gussio R (2005) A common pharmacophore for a diverse set of colchicine site inhibitors using a structure-based approach. *J Med Chem* **48:**6107–6116.

Nogales E, Wolf SG, and Downing KH (1998) Structure of the αβ tubulin dimer by electron crystallography. *Nature (Lond)* **391:**199–203.

Pettit GR, Herald CL, Boyd MR, Leet JE, Dufresne C, Doubek DL, Schmidt JM, Cerny RL, Hooper JNA, and Rutzler KC (1991) Isolation and structure of the cell growth inhibitory constituents from the Western Pacific marine sponge *Axinella* sp. *J Med Chem* **34:**3339–3340.

Pettit GR, Singh SB, Hogan F, Lloyd-Williams P, Herald DL, Burkett DD, and Clewlow PJ (1989) The absolute configuration and synthesis of natural (−)-dolastatin 10. *J Am Chem Soc* **111:**5463–5465.

Ravelli RBG, Gigant B, Curmi PA, Jourdain I, Lachkar S, Sobel A, and Knossow M (2004) Insight into tubulin regulation from a complex with colchicine and a stathmin-like domain. *Nature (Lond)* **428:**198–202.

Safa AR, Hamel E, and Felsted RL (1987) Photoaffinity labeling of tubulin subunits with a photoactive analogue of vinblastine. *Biochemistry* **26:**97–102.

Seletsky BM, Wang Y, Hawkins LD, Palme MH, Habgood GJ, DiPietro LV, Towle MJ, Salvato KA, Wels BF, Aalfs KK, et al. (2004) Structurally simplified macrolactone analogues of halichondrin B. *Bioorg Med Chem Lett* **14:**5547–5550.

Timasheff SN, Andreu JM, and Na GC (1991) Physical and spectroscopic methods for the evaluation of the interactions of antimitotic agents with tubulin. *Pharmacol Ther* **52:**191–210.

Towle MJ, Salvato KA, Budrow J, Wels BF, Kuznetsov G, Aalfs KK, Welsh S, Zheng W, Seletsky BM, Palme MH, et al. (2001) In vitro and in vivo anticancer activities of synthetic macrocyclic ketone analogs of halichondrin B. *Cancer Res* **61:**1013–1021.

Uemura D, Takahashi K, Yamamoto T, Katayama C, Tanaka J, Okumura Y, and Hirata Y (1985) Norhalichondrin A: an antitumor polyether macrolide from a marine sponge. *J Am Chem Soc* **107:**4796–4798.

Zheng W, Seletsky BM, Palme MH, Lydon PJ, Singer LA, Chase CE, Lemelin CA, Shen Y, Davis H, Tremblay L, et al. (2004) Macrocyclic ketone analogues of halichondrin B. *Bioorg Med Chem Lett* **14:**5551–5554.

Address correspondence to: Dr. Ernest Hamel, Building 469, Room 104, National Cancer Institute at Frederick, Frederick MD 21702. E-mail: hamele@mail.nih.gov